((26. 02. 2014))

Sites for Methane Activation on Li-doped MgO Surfaces [**]

Karolina Kwapien, Joachim Paier, Joachim Sauer,* Michael Geske, Ulyana Zavyalova, Raimund Horn,*† Pierre Schwach, Annette Trunschke,* Robert Schlögl

((Catch Phrase:)) **C-H activation on MgO**

* Dr. K. Kwapien, Dr. J. Paier, Prof. Dr. J. Sauer, Institut für Chemie, Humboldt-Universität, Unter den Linden 6, 10099 Berlin, Deutschland, Email: sek.qc@chemie.hu-berlin.de

Dr. M. Geske, Dr. U. Zavyalova, Prof. Dr. R. Horn, Dr. A. Trunschke, Prof. Dr. R. Schlögl, Fritz-Haber-Institut der Max-Planck-Gesellschaft, Faradayweg 4-6, 14195 Berlin, Deutschland

†Present address: Institut für Chemische Reaktionstechnik Technische Universität Hamburg-Harburg, Eißendorfer Str. 38, 21073 Hamburg, Deutschland

[**] This work has been supported by Deutsche Forschungsgemeinschaft within the Cluster of Excellence „Unifying Concepts in Catalysis“. We thank Wiebke Frandsen for recording of MgO images by transmission electron microscopy. KK thanks the International Max Planck Research School “Complex Surfaces in Materials Science” for a fellowship. JS is grateful for a Miller Visiting Professorship at Berkeley during which parts of this paper have been written.

Abstract: Density functional calculations yield energy barriers for H abstraction by oxygen radical sites in Li-doped MgO that are much smaller (12 ± 6 kJ/mol) than the barriers inferred from different experimental studies (80 – 160 kJ/mol). This raises further doubts that the $Li^+O^{\bullet-}$ site is the active site as postulated by Lunsford. From temperature programmed oxidative coupling reactions of methane (OCM) we conclude that the same sites are responsible for the activation of CH_4 on both Li-doped MgO and pure MgO catalysts. For a MgO catalyst prepared by sol-gel synthesis, the activity proved to be very different in the initial phase of the OCM reaction and in the steady state. This was accompanied by substantial morphological changes and restructuring of the terminations as transmission electron microscopy revealed. Further calculations on cluster models showed that CH_4 binds heterolytically on $Mg^{2+}O^{2-}$ sites at steps and corners, and that the homolytic release of methyl radicals into the gas phase will happen only in the presence of O_2.

Taylors active site concept[1] has stimulated catalysis research over almost a century, but it took many decades until surface science identified low-coordinated atoms at step edges as active sites of metal catalysts.[2] Subsequently, the complex nature of active sites at supported metal[3] or metal oxide catalysts[4,5] has been revealed by combined experimental and computational studies. With the raw material shift in chemical industry to natural gas, there is renewed interest in the formation of higher hydrocarbons, e.g., by oxidative coupling of methane (OCM):[6]

$$2\ CH_4 + O_2 \rightarrow C_2H_4 + 2\ H_2O. \quad (1)$$

The simplest catalysts for this reaction, among a large number of complex solid oxides, is Li-doped MgO.[7] Early, Lunsford proposed that the active sites are $O^{\bullet-}$ radicals neighbored to

Li^+, with $Li^+O^{\bullet-}$ formally replacing $Mg^{2+}O^{2-}$,[8] and that the C–H bond is activated by homolytic splitting involving hydrogen atom transfer to the $O^{\bullet-}$ sites.[9]

$$H_3C–H + [O^{\bullet-}Li^+]_{MgO} \rightarrow H_3C^{\bullet} + [HO^-Li^+]_{MgO} \quad (2)$$

However, there is also evidence that the $Li^+O^{\bullet-}$ site may not be the active site and that the C–H bond may be heterolytically split,[6] as Lunsford already mentioned in his 1995 review.[7] Recently, crucial ENDOR experiments showed that in none of the powder catalysts that were run under an OCM atmosphere Li^+O^- centers could be found,[10,11] although they were detectable in Li-doped MgO single crystals prepared by arc fusion of MgO/Li_2CO_3.[10] Instead, by careful multi-method characterization,[11,12] Li addition was found to lead to restructuring of the MgO surface exposing steps and corner sites and high-index crystallographic surfaces alien to pristine MgO. Studies of thin MgO films by surface science techniques reached the same conclusion.[10]

Here, we provide theoretical and further experimental evidence that the $Li^+O^{\bullet-}$ site is not the active site and conclude that the activity of OCM catalysts is connected with morphological features of the crystallites that form under reaction conditions and depend on the synthesis process. Lunsford already points to a discrepancy[7] between the measured apparent activation energy for the formation of methyl radicals (96±8 kJ/mol)[13] and quantum chemical calculations. In 2005 Catlow et al. used density functional theory and periodic models to calculate the energy barrier of H abstraction by an $O^{\bullet-}$ site at the (001) surface of Li-doped MgO.[14] The barrier obtained, 74 kJ/mol, more or less is in apparent agreement with the above value and reported barriers of 85 kJ/mol (CH_4/CD_4 isotope exchange)[15] and 90 kJ/mol (C2 hydrocarbon formation).[16] Microkinetic simulations yielded significantly higher values, 147 kJ/mol.[17] More recently, Li-doped MgO catalysts have been found unstable under reaction conditions, and after 24 h time on stream barriers between 89 and 160 kJ/mol have been measured, depending on the synthesis method.[18]

We report quantum chemical calculations that go beyond limitations of previous work as far as models for the active site, localization method of the transition structure and accuracy of the quantum chemical approach are concerned. Our predicted energy barriers, between 7 ± 6 and 27 ± 6 kJ/mol, are surprisingly low compared to the experimental results which suggests that the $Li^+O^{\bullet-}$ site is not the active site.

Support for this conclusion comes from temperature programmed reaction experiments, which show that on both Li-doped MgO and pure MgO catalysts conversion of CH_4 and O_2 starts at about 410 °C and formation of C2 species at about 540 °C. The difference is that in this initial phase of the reaction Li-MgO is far more active and selective in forming C2 coupling products than pure MgO. We conclude that the reaction pathways are the same for both materials and that the same active sites are present. The role of Li-doping is increasing the number of active sites, most likely due to changes of the morphology connected with the formation of a larger number of low coordinated O^{2-} ions at edges, corners, and kinks.[10-12]

For further kinetic studies a pure MgO model catalyst has been synthesized by a sol-gel process and characterized by transmission electron microscopy (TEM). The catalyst activity proved to be very different in the initial phase of the OCM reaction and in the steady state, and this was accompanied by substantial morphological changes. In steady state, the apparent activation barrier for CH_4 conversion is 133±2 kJ/mol, within the 80 to 160 kJ/mol range inferred before for Li-doped MgO.[15-18]

To further explore possible sites for CH_4 activation on Li-free MgO catalysts, we have examined the interaction of CH_4 with morphological defects (steps, corners) by DFT. The calculations showed that the C-H bond adds heterolytically onto an $Mg^{2+}O^{2-}$ pair, but that homolytic release of methyl radicals in the gas phase is only likely in the presence of O_2.

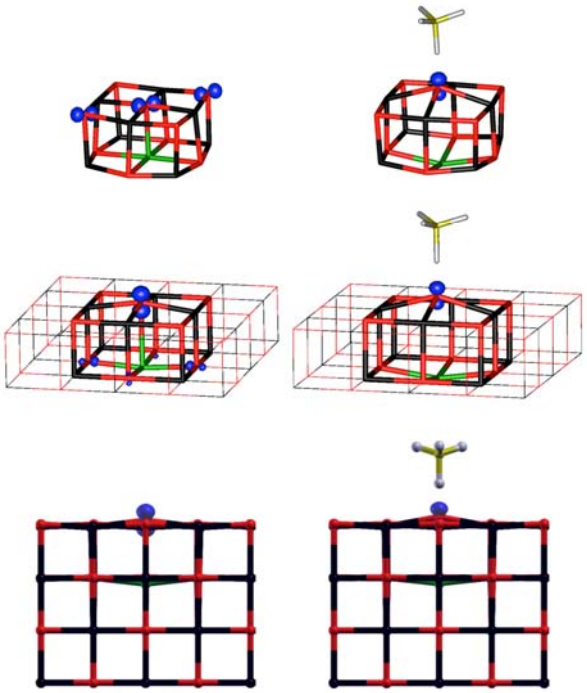

Figure 1. From top to bottom: Cluster model, constraint cluster model embedded in a periodic array of point charges, and periodic model of an $Li^{+}O^{\bullet-}$ site on the MgO(001) terrace. Left - active site structure, right - transition structure for H abstraction from CH_4. O – red, Mg – black, Li – green, C – yellow, H – gray, spin density – blue.

Figure 1 shows both cluster and periodic models adopted for the $Li^{+}O^{\bullet-}$ site at the MgO (001) surface terrace. The $LiO(MgO)_8$ cluster has the topology of a two-layer cut-out from the surface. In the constraint cluster model we limit structure relaxation to the Li^{+} and $O^{\bullet-}$ ions in the center of the cluster, whereas the positions of all other atoms are fixed at the positions they have in the MgO bulk. In our four-layer slab model all ion positions are relaxed except those in the two bottom layers. The B3LYP hybrid density functional[19,20] has been used, which reproduces within 6 kJ/mol CCSD(T) coupled cluster results of C-H bond spitting barriers for CH_4 at $O^{\bullet-}$ sites of $(MgO)_n^{\bullet+}$ clusters.[21,22] CCSD(T) is considered to be chemically accurate. For gas phase metal oxide clusters featuring radical sites, B3LYP has

also been shown to correctly predict for which clusters hydrogen abstraction can be observed by mass spectrometry and for which not.[21,23]

Table 1. Apparent energy barriers (B3LYP functional) for hydrogen abstraction from methane at $Li^+O^{\bullet-}$ sites at the MgO(001) terrace and corner sites in kJ/mol.

model	terrace	corner-1	corner-2
cluster, free	61.3	18.9	21.7
cluster, constraint[a]	57.3	22.8	22.4
cluster, embedded[a,b]	41.2 [29.3][c]	29.8	29.5
periodic model	26.8 (35.1)[d]	(23.7)[d]	(52.2)[d]
+ dispersion	12.3 (26.8)[d]	(21.8)[d]	(42.1)[d]

[a] Only the surface O ion and the Li ion beneath are allowed to move

[b] Periodic electrostatic embedded cluster model, ref.[24]

[c] Single point calculation at the B3LYP structure obtained for the periodic model

[d] Single point hybrid B3LYP(cluster):PBE(periodic) calculations at the PBE structure obtained for the periodic model

Fig. 1 shows the geometric structures of the active site and the transition state (for bond distances see supporting information) as well as the spin densities. In the transition structure the spin localizes at the surface oxygen ion above the lithium ion for all models. In the initial state, the unconstrained model shows delocalization over two additional oxygen ions. This is rectified when embedding the cluster in a periodic array of point charges and a finite number of full ion pseudopotentials, which also lowers the apparent barrier by 20 kJ/mol (Table 1, terrace). The periodic model barrier is only 14 kJ/mol lower than the embedded cluster barrier and 12 kJ/mol of this difference are due to relaxing a larger number of atoms in the periodic model. This we gather from the single point embedded cluster result at the structure obtained for the periodic model.

We conclude that for $Li^+O^{\bullet-}$ terrace sites, the activation barrier is as low as 12±6 kJ/mol (Table 1). The much higher previous estimates (74 kJ/mol)[14] we ascribe to neglect of

dispersion and an incomplete optimization for the transition structure in that study. For different morphological positions, e.g. at corners, depending on the model the barriers may be 5 kJ/mol lower ("corner 1") or 15 kJ/mol higher ("corner 2") than for terrace sites, see Table 1 (last row).

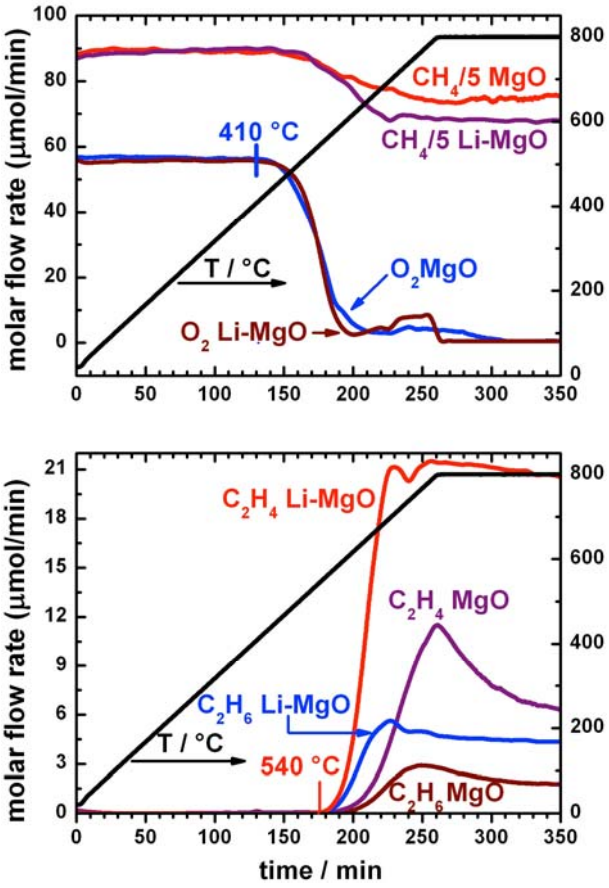

Figure 2. Flow rates of CH_4, O_2 (top), and C_2H_6, C_2H_4 (bottom) in temperature programmed oxidative methane coupling on pure MgO and 5wt% Li-doped MgO.

Temperature programmed reaction measurements were carried out on 150 mg of pure MgO and 5wt% Li-doped MgO, both prepared by gel combustion synthesis as described before.[11]

Briefly, glycerol as fuel was mixed with aqueous solutions of $LiNO_3$ and $Mg(NO_3)_2$. After water was removed by evaporation, a highly energetic, combustible gel was obtained in which Li^+ and Mg^{2+} ions were molecularly dispersed. Upon ignition the gel combusted vigorously to the oxides followed by rapid thermal quenching. Yet, despite rapid combustion and rapid thermal quenching which may lead to structures far from equilibrium, it was not possible to detect Li^+O^- defects in any material obtained this way. As discussed in detail in Ref.[11] CW-EPR, ENDOR and DR-UV/Vis, all established diagnostic methods for Li^+O^- defects,[10,25] were applied, but no method could detect Li^+O^- defects in any of our materials. Using optical spectroscopy morphological defects, i.e. low coordinated O^{2-} ions at edges, corners, and kinks of the MgO surface have been identified which arise from the volatilization of the Li component being initially present in the MgO sample as solid solution.

The pure MgO and the Li-doped MgO catalysts were subjected to a temperature ramp of 3K/min in a plug flow reactor using an OCM mixture consisting of 10 ml/min CH_4, 1.25 ml/min O_2 and 2 ml /min Ar as internal standard. Figure 2 shows the results for CH_4, O_2, C_2H_4 and C_2H_6, the corresponding data for CO and CO_2 formation are given in the Supporting Information. On both catalysts O_2 and CH_4 conversion to CO_2 commences at about 410 °C with CO_2 as the far dominant oxidation product. Arrhenius plots on O_2 consumption (cf. Supporting Information) give very similar apparent activation energies of 205 and 184 kJ/mol on pure MgO and Li-MgO, respectively, indicating a similar mechanism of initial O_2 activation on both materials. CO, C_2H_6 and C_2H_4 formation begins on both materials at 540°C, but Li-MgO is far more active and selective in forming C2 coupling products than pure MgO.

TEM investigations of MgO particles obtained by a sol-gel process show substantial morphology changes during time on stream. Figure 3 shows a TEM image of the MgO catalyst used for the data in Table 2 after 6h and after 230 h time on stream. Careful transfer

into the TEM under exclusion of air reveals the restructuring of the termination, losing the (100) orientation from the fresh MgO for a rough termination structure. In both cases substantial numbers of non-terrace sites are present that expose Mg sites with lower coordination than 5-fold and may serve as active sites. The diffuse termination of the 230 h used sample indicates the presence of additional terminating species such as –OH groups that may block many of such sites for methane adsorption.

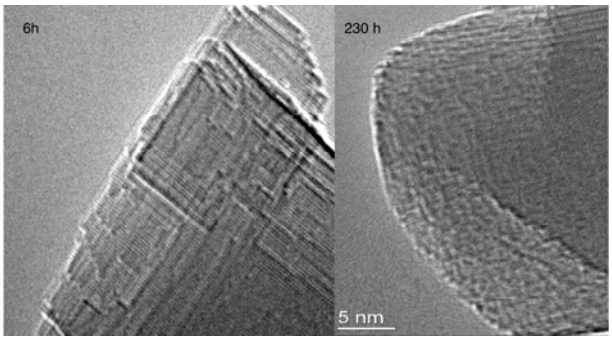

Figure 3. TEM images of pure MgO after 6h (left) and after reaching steady state (230 h, right).

Table 2. Performance of the Li free MgO catalyst in the oxidative coupling of methane, X – conversion, S(C2) – selectivity to ethane and ethylene

	rate [$\mu mol \cdot s^{-1} \cdot g_{cat}^{-1}$]	rate [$\mu mol \cdot s^{-1} \cdot m_{cat}^{-2}$]	$X(CH_4)$ [%]	$S(C_2)$ [%]
initial state	214.4	5.56	26.04	29.84
final state	8.57	1.26	4.70	13.85

Concomitantly with the morphological changes, the catalyst activity proved to be very different in the initial phase of the OCM reaction and the steady state (Table 2). CH_4 conversion and C2 selectivity changed from 26 and 30 %, respectively, to 5 and 14 %, respectively. This is connected with substantial restructuring as the rate per catalyst weight reduces by factor of 25, whereas the rate per surface area reduces by a factor of 4.4 only.

As model for morphological defects (steps, corners) on Li-free MgO catalysts we adopt the $(MgO)_9$ cluster. Figure 4 shows the energy diagram for the reaction with CH_4. Chemisorption occurs by heterolytic addition of the C-H bond onto an $Mg^{2+}O^{2-}$ pair,

$$[Mg^{2+}O^{2-}]_{MgO} + H{-}CH_3 \rightarrow [HO^{-}(Mg{-}CH_3)^{+}]_{MgO} \rightarrow [HO^{-}Mg^{\bullet+}]_{MgO} + {}^{\bullet}CH_3 \qquad (3)$$

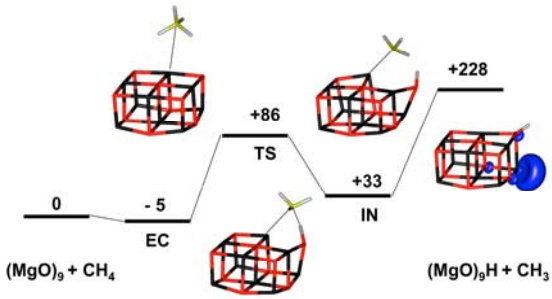

Figure 4. Reaction energy diagram for chemisorption of CH_4 onto corner/edge sites of a Mg_9O_9 cluster showing C-H bond addition on an $Mg^{2+}O^{2-}$ pair. B3LYP energies are given in kJ/mol, for energies including zero-point vibrational contributions see Supporting Information. EC – encounter complex, TS transition state, IN intermediate; colors as in Fig.1.

The surface species formed are a hydroxyl group (by protonation of O^{2-}) and a Grignard type Mg-methylate (by adding CH_3^- to Mg^{2+}). Such reactions have been discussed before,[26] e.g., for low coordinated sites on γ-alumina.[27] The barrier for this slightly endothermic reaction is at the low side of typical barriers for OCM reactions, but releasing a methyl radical to the gas phase is barrierless but needs as much as 228 kJ/mol. However, the unpaired electron formed in this reaction, facilitates O_2 chemisorption as a superoxide species,

$$[HO^{-}Mg^{\bullet+}]_{MgO} + O_2 \rightarrow (O_2^{\bullet-})[HO^{-}Mg^{2+}]_{MgO} \qquad (4)$$

This process is very exothermic (-191 kJ/mol, see also ref.[28]), so that the overall process,

$$[Mg^{2+}O^{2-}]_{MgO} + H{-}CH_3 + O_2 \rightarrow (O_2^{\bullet-})[HO^{-}Mg^{2+}]_{MgO} + {}^{\bullet}CH_3 \quad (5)$$

becomes almost thermal neutral (ΔE = 37 kJ/mol). There is, of course, an entropy penalty since two gas phase species are converted into one, but reaction (5) yields also a superoxo surface species that is more reactive than O_2 in the gas phase.

Future studies should also consider possible reactions of dioxygen with the Mg-methylate which may also lead to methyl radicals and surface peroxo species, see, e.g., refs. [29,30]. Pros and cons of reaction (5) as a possible source of methyl radicals in the OCM process have already been discussed in ref. [7] Our model calculations are indeed strong evidence that heterolytic chemisorption of CH_4 on MgO in the presence of O_2, becomes energetically feasible on morphological defects such as steps or corners and plays a significant role in the OCM process. Currently, we are further investigating possible mechanisms based on this idea. Whereas quantum chemical calculations on realistic models as presented here can provide reliable information on individual reaction steps, comparison with experimental kinetic data requires micro-kinetic simulations that use these data as input.

Our experiments (see also ref.[31]) in combination with theoretical studies suggest a different role of non-reducible oxides as catalysts on methane activation. Their role is not to provide and receive back electrons as with reducible oxide catalysts, but merely to stay inert with its own electronic system and just bring together the reactants allowing exchanging redox equivalents directly between themselves. Such a function is expressed in the designation "catalyst" meaning the bringing together of reactants.

Received: ((will be filled in by the editorial staff))

Published online on ((will be filled in by the editorial staff))

Keywords: active site · C-H activation · density functional calculations · Li-doped MgO · magnesium oxide

[1] H. S. Taylor, *Proc. R. Soc. London Ser. A* **1925**, *108*, 105-111.

[2] T. Zambelli, J. Wintterlin, J. Trost, G. Ertl, *Science* **1996**, *273*, 1688-1690.

[3] M. Behrens, F. Studt, I. Kasatkin, S. Kühl, M. Hävecker, F. Abild-Pedersen, S. Zander, F. Girgsdies, P. Kurr, B.-L. Kniep, M. Tovar, R. W. Fischer, J. K. Nørskov, R. Schlögl, *Science* **2012**, *336*, 893-897.

[4] M. V. Ganduglia-Pirovano, C. Popa, J. Sauer, H. L. Abbott, A. Uhl, M. Baron, D. Stacchiola, O. Bondarchuk, S. Shaikhutdinov, H.-J. Freund, *J. Am. Chem. Soc.* **2010**, *132*, 2345-2349.

[5] K. Amakawa, L. Sun, C. Guo, M. Hävecker, P. Kube, I. E. Wachs, S. Lwin, A. I. Frenkel, A. Patlolla, K. Hermann, R. Schlögl, A. Trunschke, *Angew. Chem., Int. Ed.* **2013**, n/a-n/a.

[6] E. V. Kondratenko, M. Baerns in *Handbook of Heterogeneous Catalysis*, *Vol. 6* (Ed. H. K. G. Ertl, F. Schüth, J. Weitkamp), Wiley-VCH, **2008**.

[7] J. H. Lunsford, *Angew. Chem., Int. Ed.* **1995**, *34*, 970-980.

[8] D. J. Driscoll, W. Martir, J. X. Wang, J. H. Lunsford, *J. Am. Chem. Soc.* **1985**, *107*, 58 - 63.

[9] T. Ito, J. Wang, C. H. Lin, J. H. Lunsford, *J. Am. Chem. Soc.* **1985**, *107*, 5062-5068.

[10] P. Myrach, N. Nilius, S. V. Levchenko, A. Gonchar, T. Risse, K. P. Dinse, L. A. Boatner, W. Frandsen, R. Horn, H. J. Freund, R. Schlögl, M. Scheffler, *ChemCatChem* **2010**, *2*, 854-862.

[11] U. Zavyalova, G. Weinberg, W. Frandsen, F. Girgsdies, T. Risse, K. P. Dinse, R. Schloegl, R. Horn, *ChemCatChem* **2011**, *3*, 1779-1788.

[12] U. Zavyalova, M. Geske, R. Horn, G. Weinberg, W. Frandsen, M. Schuster, R. Schlögl, *ChemCatChem* **2011**, *3*, 949-959.

[13] M. Xu, C. Shi, X. Yang, M. P. Rosynek, J. H. Lunsford, *J. Phys. Chem.* **1992**, *96*, 6395-6398.

[14] C. R. A. Catlow, S. A. French, A. A. Sokol, J. M. Thomas, *Philos. Trans. Royal Soc. Ser. A* **2005**, *363*, 913-936.

[15] V. S. Muzykantov, A. A. Shestov, H. Ehwald, *Catal. Today* **1995**, *24*, 243-244.

[16] M. Y. Sinev, V. Y. Bychkov, V. N. Korchak, O. V. Krylov, *Catal. Today* **1990**, *6*, 543-549.

[17] J. Sun, J. W. Thybaut, G. B. Marin, *Catal. Today* **2008**, *137*, 90-102.

[18] S. Arndt, U. Simon, S. Heitz, A. Berthold, B. Beck, O. Görke, J. D. Epping, T. Otremba, Y. Aksu, E. Irran, G. Laugel, M. Driess, H. Schubert, R. Schomäcker, *Top. Catal.* **2011**, *54*, 1266-1285.

[19] A. D. Becke, *J. Chem. Phys.* **1993**, *98*, 5648-5652.

[20] C. Lee, W. Yang, R. G. Parr, *Phys. Rev. B* **1988**, *37*, 785-789.

[21] K. Kwapien, M. Sierka, J. Döbler, J. Sauer, *ChemCatChem* **2010**, *2*, 819-826.

[22] K. Kwapien, Active Sites for Methan Activation in MgO and Li-doped MgO, Doctoral thesis, Humboldt University, 2011.

[23] S. Feyel, J. Döbler, R. Höckendorf, M. K. Beyer, J. Sauer, H. Schwarz, *Angew. Chem., Int. Ed.* **2008**, *47*, 1946-1950.

[24] A. M. Burow, M. Sierka, J. Döbler, J. Sauer, *J. Chem. Phys.* **2009**, *130*, 174710.

[25] M. M. Abraham, Y. Chen, L. A. Boatner, R. W. Reynolds, *Phys. Rev. Lett.* **1976**, *37*, 849-852.

[26] C. Copéret, *Chem. Rev.* **2010**, *110*, 656-680.

[27] R. Wischert, P. Laurent, C. Copéret, F. Delbecq, P. Sautet, *J. Am. Chem. Soc.* **2012**, *134*, 14430-14449.

[28] D. Ricci, G. Pacchioni, P. V. Sushko, A. L. Shluger, *Surf. Sci.* **2002**, *542*, 293-306.

[29] A. G. Davies, B. P. Roberts, *Acc. Chem. Res.* **1972**, *5*, 387-392.

[30] P. J. Bailey, R. A. Coxall, C. M. Dick, S. Fabre, L. C. Henderson, C. Herber, S. T. Liddle, D. Loroño-González, A. Parkin, S. Parsons, *Chem. Eur. J.* **2003**, *9*, 4820-4828.

[31] P. Schwach, W. Frandsen, M. Willinger, R. Schlögl, A. Trunschke, *in preparation* **2013**.